Author's Accepted Manuscript

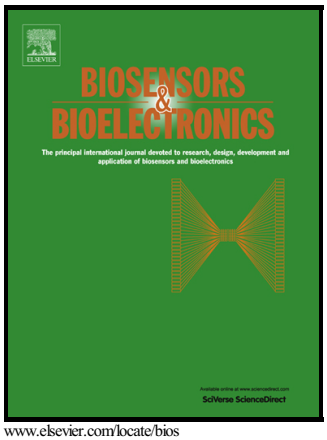

www.elsevier.com/locate/bios

Microelectrospotting as a new method for electrosynthesis of surface-imprinted polymer microarrays for protein recognition

Maria Bosserdt, Júlia Erdőssy, Gergely Lautner, Julia Witt, Katja Köhler, Nenad Gajovic-Eichelmann, Aysu Yarman, Gunther Wittstock, Frieder W. Scheller, Róbert E. Gyurcsányi

PII: S0956-5663(15)30147-0
DOI: http://dx.doi.org/10.1016/j.bios.2015.05.049
Reference: BIOS7713

To appear in: *Biosensors and Bioelectronic*

Received date: 28 April 2015
Accepted date: 22 May 2015

Cite this article as: Maria Bosserdt, Júlia Erdőssy, Gergely Lautner, Julia Witt, Katja Köhler, Nenad Gajovic-Eichelmann, Aysu Yarman, Gunther Wittstock, Frieder W. Scheller and Róbert E. Gyurcsányi, Microelectrospotting as a new method for electrosynthesis of surface-imprinted polymer microarrays for protein recognition, *Biosensors and Bioelectronic,* http://dx.doi.org/10.1016/j.bios.2015.05.049

Microelectrospotting as a new method for electrosynthesis of surface-imprinted polymer microarrays for protein recognition

Maria Bosserdt[a], Júlia Erdőssy[b], Gergely Lautner[b], Julia Witt[d], Katja Köhler[a], Nenad Gajovic-Eichelmann[a], Aysu Yarman[a], Gunther Wittstock[d], Frieder W. Scheller[a], Róbert E. Gyurcsányi[b,d*]

[a]Fraunhofer Institute IZI-BB, D-14476 Potsdam, Germany

[b]Research Group for Technical Analytical Chemistry, Department of Inorganic and Analytical Chemistry, Budapest University of Technology and Economics, Szt. Gellért tér 4, H-1111 Budapest, Hungary

[c]MTA-BME "Lendület" Chemical Nanosensors Research Group, Department of Inorganic and Analytical Chemistry, Budapest University of Technology and Economics, Szent Gellért tér 4, H-1111 Budapest, Hungary, E-mail: robertgy@mail.bme.hu

[d]Carl von Ossietzky University of Oldenburg, Department of Chemistry, D-26111 Oldenburg, Germany

Keywords: molecularly imprinted polymers, surface imprinting, electrospotting, ferritin, scopoletin, electropolymerization

Abstract

Here we introduce microelectrospotting as a new approach for preparation of protein-selective molecularly imprinted polymer microarrays on bare gold SPR imaging chips. During electrospotting both the gold chip and the spotting tip are electrically connected to a potentiostat as working and counter electrodes, respectively. The spotting pin encloses the monomer-template protein cocktail that upon contacting the gold surface is *in-situ* electropolymerized resulting in surface confined polymer spots of ca. 500 µm diameter. By repeating this procedure at preprogrammed locations for various composition monomer-template mixtures microarrays of nanometer-thin surface-imprinted films are generated in a controlled manner. We show that the removal and rebinding kinetics of the template and various potential interferents to such microarrays can be monitored in real-time and multiplexed manner by SPR imaging. The proof of principle for microelectrospotting of electrically insulating surface-imprinted films is made by using scopoletin as monomer and ferritin as protein template. It is shown that microelectrospotting in combination with SPR imaging can offer a versatile platform for label-free and enhanced throughput optimization of the molecularly imprinted polymers for protein recognition and for their analytical application.

1. Introduction

While the use of molecular imprinting to prepare selective synthetic sorbents (Dickey 1949) for small molecular weight compounds is now well established and in many respects seem to reach its limits, efforts are redirected to prepare molecularly imprinted polymers (MIPs) for macromolecules, in particular proteins(Ge and Turner 2008; Whitcombe et al. 2011). Such MIPs are intended to fulfil the promises formulated at the early launching of the field (Vlatakis et al. 1993), i.e., to enable the preparation of "plastic antibodies". Owing to their fully synthetic preparation and robustness MIP-based artificial receptors are expected to have a major impact on chemical sensing, catalysis and separation (Chen et al. 2011; Wulff and Liu 2012). However, new applications of protein MIPs are also emerging such as their use to facilitate protein crystallization (Saridakis et al. 2011) or to prepare selective artificial enzyme inhibitors (Zheng et al. 2013). Proteins as large template molecules rich in functionalities are expected to provide MIPs with higher binding affinities than those obtained by imprinting small molecular weight compounds. On the other hand, such a richness in functionality may lead to imprints with cross reactivity to other compounds. Additionally, the larger mass of protein templates as well as their structural mobility render the synthesis of protein MIPs difficult in terms of generating, accessible and highly selective binding sites. Therefore, despite some very convincing particular applications (Cai et al. 2010), the development of a simple universal synthetic approach for fabrication of MIPs with selective protein recognition capabilities seems to be overly optimistic. Thus, a more gradual strategy is required to overcome step-by-step the essential problems in the development of highly selective protein MIPs. In this respect the implementation of epitope imprinting, (Nishino et al. 2006; Rachkov and Minoura 2000) novel polymerization techniques and functional monomers (Yildirim et al. 2012), as well as surface imprinting (Hayden et al. 2006a; Hayden et al. 2006b; Kempe et al. 1995; Shi et al. 1999) are important milestones towards a universal synthetic approach. We have focused in particular on surface imprinting technologies to overcome the limitations imposed by the small diffusivity of proteins in the highly cross-linked MIP structures, by generating binding sites exclusively on the surface of the MIPs(Menaker et al. 2009) and simultaneously providing high surface area/volume MIP micro- or nanostructures (Bognár et al. 2013; Ceolin et al. 2013; Lautner et al. 2011). However, the development of protein MIPs would have to benefit clearly from high throughput synthesis and testing methodologies as commonly used in development of various bioreceptors, e.g., aptamers (Szeitner et al. 2014).Therefore, here we propose microelectrospotting as a new methodology to prepare by electrosynthesis arrays of surface-imprinted polymers for protein recognition on bare gold surface plasmon resonance imaging (SPRi) chips. Microelectrospotting is expected to enable the fabrication of surface imprinted MIP arrays for different protein templates by using different experimental conditions, e.g. different concentrations and ratios of monomer and template. The application of electrospotting for the electrosynthesis of MIP arrays is unprecedented. Certainly, to take advantage of the MIP microarray format a multiplexed readout methodology is required as SPR imaging, which offers the opportunity for *simultaneous* label-free determination of the binding properties of the respective MIP spots in a high throughput manner. The

main advantage of this approach over other electrosynthesised MIPs (Yu and Lai 2005) is that the electrospotted MIP microarrays enables both the optimization of the protein MIP electrosynthesis on a single chip as well as the fabrication of MIP arrays for different proteins.

Until now electrospotting as a mean for microarray fabrication was used only for immobilization, i.e., to immobilize pyrrole labelled biomolecules (oligonucleotide, peptide, proteins and oligosaccharides) (Mercey et al. 2007; Villiers et al. 2009) onto SPRi chips with higher stability than classical self-assembled monolayer-based immobilization methods (Guedon et al. 2000). The biomolecules were coupled through a very thin polymeric layers of less than 10 nm to enable properly sensitive SPR monitoring of target binding to the attached biomolecules. For protein imprinting purposes such thin films can be considered inherently surface imprinted as their thickness is comparable with the hydrodynamic radius of the template proteins. Consequently, we expected that the microelectrospotting will enable the free exchange of proteins between the MIP and sample solution and concurrently the label-free, *in situ* monitoring of the binding kinetics on MIP arrays by using SPRi. While microelectrospotting as a mean for microarray fabrication was demonstrated only for pyrrole-derivatives leading to electrically conductive films, here we introduce the microelectrospotting for the preparation of electrically insulating surface-imprinted polymer films by electropolymerization of scopoletin monomer in the presence of ferritin. Scopoletin was chosen as a monomer because as we shown previously the thickness of the film can be controlled with ca. 1 nm precision and was found to provide MIPs with high selectivity and imprinting factor for cytochrome C (Dechtrirat et al. 2012) and concanavalin A (Dechtrirat et al. 2014). For proof of principle we made electrospotting pins from conventional plastic micropipette tips of 10 µL volume that integrate a Ag/AgCl wire as reference/counter electrode. In the proposed configuration the gold film on the SPR chips acts as a working electrode while the monomer and protein mixture is contained by the electrically connected plastic tip. After the tip touches the gold surface a potential program is applied to electropolymerize the scopoletin onto the surface in predefined locations.

2. Materials and methods

2.1. Chemicals and reagents

Scopoletin (7-Hydroxy-6-methoxycoumarin), BSA (Bovine Serum Albumin), Ferritin from equine spleen, Urease from *Canavalia ensiformis* (jack-beans), Myoglobin and cytochrome c (Cyt c) from equine heart, as well as HS-TEG ((1-mercaptoundec-11-yl)tetra(ethylene glycol)) were purchased from Sigma (Germany). Ultrapure water of 18.2 M Ω·cm resistivity (Sartorius) and analytical grade salts were used to prepare for all aqueous solutions.

2.2. Preparation of MIP-Microarrays on gold SPR chips by microelectrospotting

For microelectrospotting a 10 µL polypropylene micropipette tip (epTIP 0.5-20 ul; Eppendorf, Hamburg, Germany) integrating a Ag/AgCl wire acting as a counter electrode was used. To prepare this electrospotting pin the side wall of the tip was pierced and the ca. 500 µm thick Ag/AgCl wire was inserted to reach inside at ca. 2 mm from the tip opening and then the hole around the wire was sealed with melted Parafilm M®. The tip was filled with freshly prepared monomer cocktail containing, unless otherwise specified, an aqueous solution of 1 mmol L^{-1} scopoletin and various concentrations of ferritin (5 µmol L^{-1}, 10 µmol L^{-1} and 25 µmol L^{-1}) in 10 mmol L^{-1} NaCl. The tip was then moved to a precise location on the gold SPR chip acting as the working electrode. The electrodes were connected to a Reference 600 potentiostat (Gamry Instruments, Warminster, PA, USA). During microelectrospotting the monomer cocktail was electropolymerized by using a potential pulse program involving a number of cycles in which the electrode is polarized at 0 V for 1 s and 0.9 V for 0.1 s. The thickness of the polymer film was controlled based on the electrical charge passed during electropolymerization. After the polymer spot was formed, the spotting tip was withdrawn and rinsed with water, and the substrate was repositioned for the next spot using a motorized stage (Newport). Repeating the microelectrospotting at different locations with different proteins at different concentrations resulted in a protein/MIP-Microarray with ca. 500 µm diameter spots. After the MIP microarray was prepared, the chip was rinsed with water to remove the unreacted monomers. In order to reduce non-specific protein adsorption to the remaining free gold surface, these areas were blocked by incubating the chip for 30 min in 1 mM (11-mercaptoundecyl)tetra(ethylene glycol) in PBS buffer (10 mM, pH 7.4) followed by rinsing with water and drying with a stream of nitrogen. As control, non-imprinted polymer (NIP) spots were prepared in the same conditions as the ferritin-MIPs but without ferritin in the monomer cocktail. For selectivity measurements BSA or Urease-imprinted polymer spots were also prepared and pretreated in the same way.

2.3. SPR experiments

For SPR measurements SPRi Flex II (HORIBA Jobin Yvon, Palaiseau, France) and Flexchip (Biacore, Uppsala, Sweden) surface plasmon imaging systems were used. These systems enable SPR chips to be prepared in an array format providing SPR information simultaneously from each spot. The simultaneous recording of the SPR signal was generally done on 36 polymer spots and four reference spots for each chip. For background correction the HS-TEG modified gold surface was used. The SPR experiments were done in a 46 µl flow cell thermostated at 25 ° C. Samples of 1.6 ml were injected into the flow cell at a flow rate of 500 µl/min. The SPR chip with the MIP microarray was mounted into the flow cell of the SPRi system and the signal was monitored in real-time. After the stabilization of the baseline in10 mM HEPES buffer (pH7.4) samples of 1.6 ml were pumped through the flow cell at a flow rate of 500 µl/min. Five mM NaOH was injected to remove the template for 20 min followed by ultrapure water for another 20 min. After that HEPES buffer was flown to until the baseline stabilized. The rebinding of the ferritin and other proteins to the MIP or NIP microspots was done in

cycles involving 20 min association, 20 min dissociation, and two consecutive regeneration steps with 5 mM NaOH and water for altogether 40 min.

2.4. Atomic force microscopic investigation of the polymer spots

Atomic force microscopy (AFM) was performed under ambient conditions with a Nanoscope IIIA controller and a Dimension 3100 stage (Veeco Instruments Inc., Santa Barbara, CA, USA) operating in two different modes. Topographical images with a resolution of 256×256 pixel were collected in the Tapping mode at a scan rate of 1.5-3.0 Hz using an Al-coated Si_3N_4-cantilever (Bruker, NCHV-A tip) with a spring constant of 42 N/m. Thickness determination were conducted in the contact mode with triangular Au-coated Si_3N_4-cantilever (Bruker, MSCT tip) of a nominal spring constant of 0.6 N/m. For this purpose an area of 1×1 μm^2 was scanned by AFM at a set-point of 10 V causing a local abrasion of the soft material until the typical structure of the gold substrate became visible. Subsequently, a topographic image of the scratched region using low forces (set points between 0 and 1 V) was recorded at 4 Hz. The thickness was determined as the difference between averaged height values between the red markers vs. the area between the green markers (Fig. S3 in supporting information). Image flattening was performed for Fig. 4 with the first order, least-square polynomial of the software Nanoscope V5.30r3sr3, which removes tilt and the vertical Z-offset between lines scans. Typical object heights (listed in in Table S1) of the main manuscript were extracted from line scans given in Figure S4. For AFM measurements the MIP was deposited on flat gold disc electrodes using the same pulse regime as for their preparation on SPR chips. The MIPs were incubated in 5 mM NaOH for 20 min to remove the template. Rebinding of the target was performed by incubating the MIP-covered electrode in 10 mM HEPES containing 150 mM NaCl and 500 nM ferritin for 30 min.

3. RESULTS AND DISCUSSION

3.1. Microelectrospotting of polymer films

The spotting pin, loaded with 10 microliter of monomer solution (with or without the protein template) was placed on a gold SPR chip surface which was polarized as working electrode (Figure 1a) against the Ag/AgCl reference. At the applied potential of 0.9 V the scopoletin monomer was oxidized to form a thin insulating polymer film over an area delimited by the micropipette tip. We used a potentiostatic pulse program for the electropolymerization, which was found to enhance the integration of slow diffusing proteins in the polymer film (Menaker et al. 2009; Schuhmann 1998). The current-time curves of the potentiostatic pulse deposition showed current peaks in response to the potential pulses which decreased gradually within the first 25 pulses reaching an almost constant value. As the amount of polymer deposited is proportional to the charge passed during the electropolymerization the current peaks were integrated to characterize the amount of film deposited. This procedure was then repeated at different positions while the composition of the monomer-protein mixture was exchanged to obtain

microarrays of surface-imprinted nanometer-thin polymer spots with different properties (Figure 1b). The chip was then inserted in the SPR imaging instrument that allows to monitor the rebinding experiments in a label-free manner at each spot.

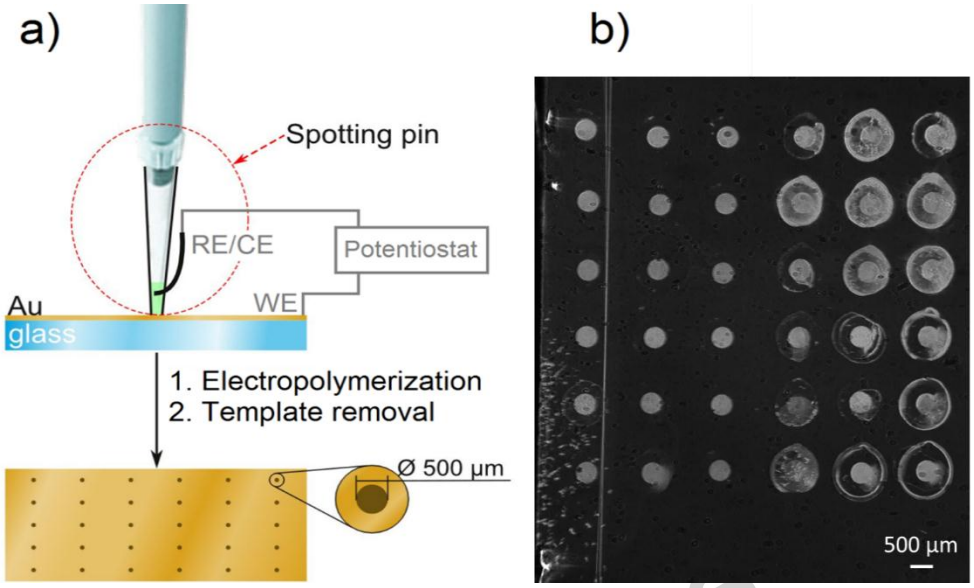

Fig. 1 (a) Schematic of the microelectrospotting method and (b) SPR image of an array of non-imprinted (left 3 columns) and ferritin-imprinted scopoletin polymer spots (with different ferritin concentrations- right 3 columns). (Supplementary Information)

The thickness of the polymer film was optimized in order to incorporate as much of the template as possible without irreversibly entrapping it in the polymer matrix. As a compromise between the lower stability of thin layers and the restriction of target accessibility with increasing thickness, 200 pulses have been chosen for the electrospotting of ferritin-imprinted MIPs. As visible in Fig. 1b the area of the MIP spots with the spotting pin used in the present study is larger than those of the NIPs, i.e. the growth of the NIP films is confined to the inner diameter of the pipette tip while the MIP extends to the outer diameter. Since the only difference between the spotted cocktail is the protein content, it is likely that the tip/surface contact area is wetted by the proteins adsorbed on the respective surfaces. For evaluation we used the centre of the polymer spots in all instances. The electrospotted film thicknesses as determined by AFM were 6 nm for NIP and 20 nm for MIP containing the template. The latter value decreased to 10-12 nm upon removal of the ferritin template. Given the experimentally determined hydrodynamic radius of 8.7 nm for ferritin this suggests that only a fraction of the ferritin molecule is imprinted in the polymer layer. For reference after 400 cycles the MIP film thickness grew to 34 nm and the NIP to ca. 10 nm.

The permeability of the polyscopoletin films was studied by CVs in solutions of a positively and a negatively charged small molecular weight redox marker in a 150 mM NaCl supporting electrolyte. Whilst the characteristic redox peaks of the positively charged ruthenium hexamine complex were not

influenced by the presence of a polyscopoletin layer on the gold electrode (Supporting information, Fig. S1), the peaks of the negatively charged ferro-/ferricyanide system were completely suppressed. Thus the polyscopoletin film is negatively charged.

3.2. Optimization of the regeneration and rebinding conditions

In order to remove the template from the MIP films, regeneration solutions able to break up different non-covalent interactions were tested. The H-bond disrupting glycine-HCl solution (10 mM, pH 2.0) did not affect the polymer spots, as shown by their unchanged sensorgrams. Injection of surfactant solution (0.05% Tween 20) led to an increase in the sensor signals of both MIP and NIP spots, presumably caused by the adsorption of Tween 20 molecules on the polymer surfaces (data not shown). Finally, treatment with 5 mM NaOH solution resulted in the desired signal decrease on the MIP spots, corresponding to the removal of the template molecules from the film (Fig. 2). The alkaline regeneration solution had only a negligible effect on the non-imprinted polymer. The signal decrease observed on the MIPs was more pronounced with increasing template concentration in the polymerization mixture. This result shows that increasing the template concentration in the polymerization mixture effectively increases the amount of protein incorporated in the MIP network.

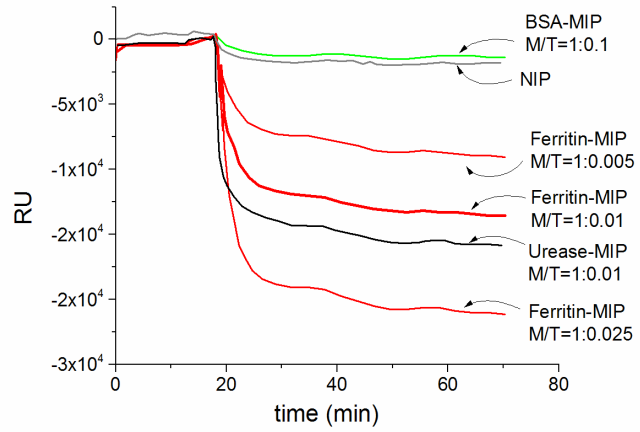

Fig. 2 Template removal with 5 mM NaOH solution from electrospotted polymer films imprinted with different concentrations and types of template proteins. The polymers were microelectrospotted by using 200 pulses from solutions containing 1 mM scopoletin in 10 mM NaCl without protein (NIP), or with target proteins (BSA, ferritin or urease). The monomer/target ratio (M/T) is indicated in the figure legend.

Rebinding experiments were carried out in HEPES buffer (10 mM, pH 7.4). Since ferritin has an isoelectric point of pH 4.5, it is negatively charged at this pH, and therefore an electrostatic repulsion is expected between the protein and the negatively charged polyscopoletin layer. This was confirmed

by a negligible SPR signal upon addition of ferritin in diluted pH 7.4 HEPES buffer. However, when the binding experiments were performed at increased ionic strength, established by adding NaCl to the HEPES buffer, a pronounced increase in the SPR signal was observed, which reached steady-state within 25 minutes, corresponding to the binding of ferritin to the MIP spots. The shielding of electrostatic repulsion was found to be already sufficient at 150 mM NaCl, but increasing the ionic strength promoted further the binding of ferritin to the MIP spots (Fig. 3).

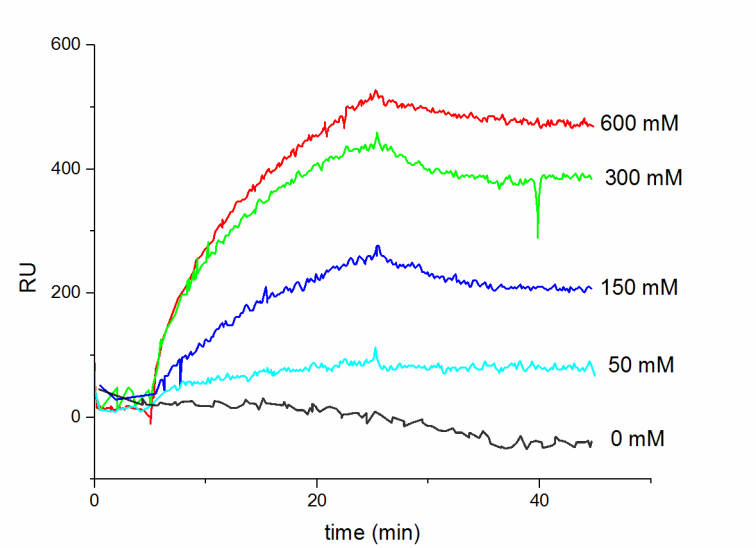

Fig. 3 Influence of the NaCl concentration (ionic strength) on the binding of ferritin to ferritin-imprinted polyscopoletin spots (M/T=1:0.025). The SPR response is shown for the injection of 500 nM ferritin in 10 mM HEPES (pH 7.4) buffer with various NaCl concentrations as indicated. The sensorgrams were corrected by substraction of the NIP signal. The coefficient of variation for the SPR signal for ferritin binding was determined from 6 parallel measurements to be ca. 5%.

On the non-imprinted polymer, however, practically no binding of ferritin was observed up to a salt concentration of 600 mM (SI, Fig. S2). At an even higher ionic strength, binding occurred on the NIP spots as well, probably due to structural changes of the protein. The highest ratio of ferritin bound on the MIP *versus* on the NIP (i.e. the imprinting factor) was obtained at 300 mM NaCl concentration. This optimal imprinting factor reached the value of 13 which is among the highest reported in the literature of protein MIPs.

3.3. AFM investigation of the MIP and NIP spots

The release and re-uptake of ferritin by MIP spots was also investigated by AFM. Figure 4 shows AFM images of polyscopoletin NIP, ferritin-imprinted polyscopoletin as prepared and after removal and reuptake of ferritin. The morphology seen for the NIP (Fig. 4a) is that of the underlying polycrystalline Au substrate on which electropolymerization of scopoletin forms a conformal film of 6 nm thickness (Table 1).

Table 1. Film thickness, roughness values (Ra) and height of typical structures for different polyscopoletin films. The relevant AFM measurements are provided in the Supporting Information.

Sample	Thickness [nm]	Roughness Ra [a] [nm]	Object heights [b] [nm]
i) polyscopoletin NIP	6.0	1.36	5.6, 3.6, 4.3
ii)ferritin-imprinted polyscopoletin (MIP)	18.1	3.29	13.7, 15.4, 8.7
iii) sample ii) after removal of ferritin	9.3	1.41	7.5, 3.6, 5.5
iv) sample iii) after reuptake of ferritin	9.7	2.57	11.9, 16.8, 9.8

[a)] Ra values were determined for an 1×1 μm^2 image frame

[b)] Figs. S3,S4

If the polyscopoletin film is prepared in presence of ferritin (MIP), a completely different film morphology is obtained (Fig. 4b). Elevated structures are clearly visible and the representative objects have dimensions similar to ferritin (Table 1). The layer thickness is about 12 nm higher than that of the NIP. This tentative assignment of the elevated structures to ferritin molecules (or clusters of them) is confirmed by the AFM image after removal of ferritin in 5 mM NaOH for 20 min which leads to a film morphology that is quite similar to that of the NIP (Fig. 4c). Also the film thickness (Table 1) decreases substantially indicating that the ferritin molecules are only partially embedded in the poly-scopoletin matrix and as such can be released into the solution. Some depressions are visible and might originate from shallow voids in the film. Given the convolution of surface morphology with the AFM tip shape, the identification of depressions cannot be further substantiated. After exposure of the sample to a 500 nM ferritin solution for 30 min (Fig. 4d), a surface morphology similar to the original MIP is observed although the average film thickness increases only slightly (Table 1). However, the size of representative objects is again in the range of ferritin molecules (Table 1). The number of attached objects seems to be smaller than in Fig. 4b which explains the lower average film thickness in comparison to the original MIP. The lower number of re-bound ferritin is reasonable because at 500 nM solution concentration only half of the saturation is reached (see Fig. 5A) and it is unlikely that each binding site is reoccupied in the uptake process.

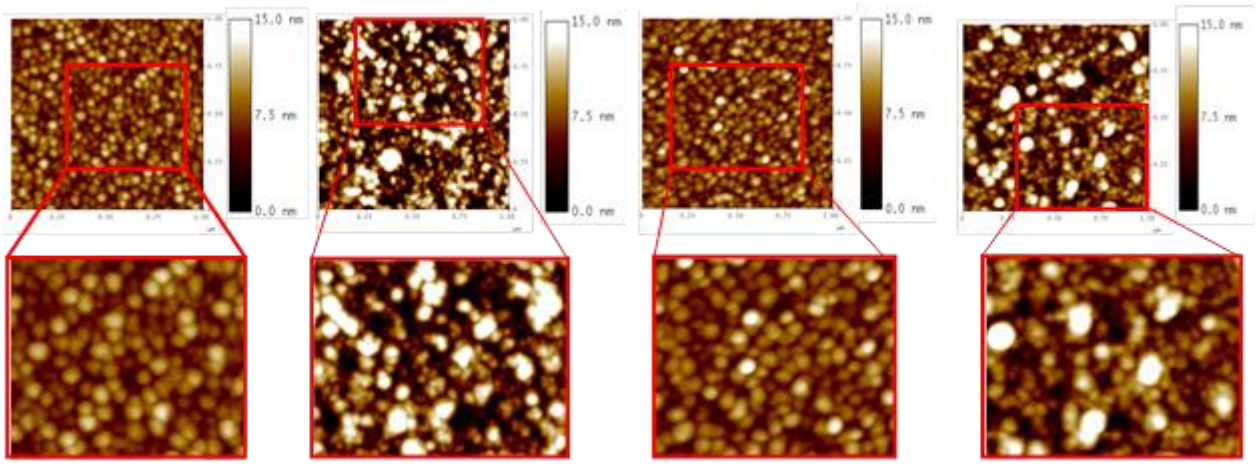

Fig. 4 AFM images of a) non-imprinted polyscopoletin, b) polyscopoletin imprinted with ferritin (M/T=0.001), c) imprinted polyscopoletin after removal of ferritin by 5 mM NaOH for 20 min; d) sample of c) after rebinding from 500 nM ferritin solution for 30 min.

3.4. Ferritin rebinding

The concentration dependence of ferritin rebinding to the imprinted polyscopoletin film was evaluated in the presence of 600 mM NaCl. Injection of the target resulted in an increase of the SPR signal which approached steady-state within 10-20 min in the case of ferritin concentrations below 0.5 µM. The injection of higher concentrations lead to a prolonged association phase and steady-state was not achieved in the time frame allowed for the measurement.

MIP spots with different M/T ratios were prepared by microelectrospotting to determine the optimal amount of the protein template in the monomer cocktail. For all different MIP spots the SPR signal increased with the ferritin concentration and approached saturation above 0.5 µM (Fig. 5A). Very importantly, NIPs and MIPs imprinted with other templates (urease or BSA) showed very low binding of ferritin under identical conditions, which confirms that selective sites are formed during microelectrospotting of polyscopoletin in the presence of ferritin. Higher ferritin concentrations during the electropolymerization resulted in larger response in both the linear and saturation region of the binding isotherm. This indicates that the number of binding sites is influenced in the studied concentration range by the amount of template during MIP formation

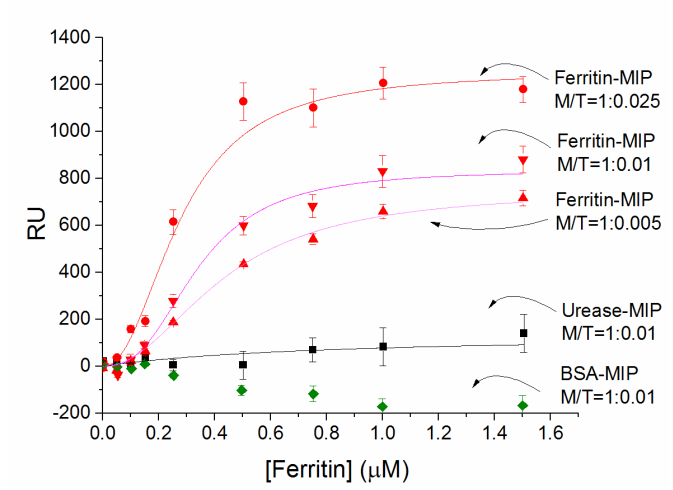

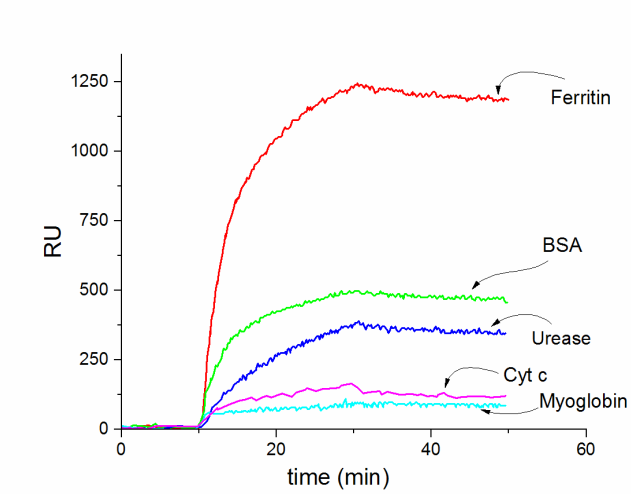

Fig. 5 (**A**) Binding isotherms of ferritin on different template imprinted polymers, measured by SPR in 10 mM HEPES pH 7.4 with 600 mM NaCl, at 25°C. Solid line are fitted Hill functions. (**B**) Typical SPR sensorgrams of ferritin-imprinted polymer spots (M/T=1:0.025) obtained upon injections of different proteins (500 nM) in 10 mM HEPES (pH 7.4) containing 600 mM NaCl.

3.5. Cross reactivity of the protein imprinted-spots

The selectivity of the polyscopoletin MIP towards its template was investigated by injecting 500 nM solutions of different proteins. The obtained sensorgrams show that the ferritin target gives the highest binding signal as shown in Fig. 5B. The ferritin-imprinted MIP shows cross-reactivity to similarly negatively charged proteins, such as urease (pI 5.0; MW 545 kDa) and BSA (pI 4.8; MW 66k Da). However, the SPR signal change is only 30 % of that of ferritin. The relatively high cross reactivity of the ferritin-imprinted MIP towards BSA is probably caused by the fact that the BSA molecule can interact via its tryptophan residues with the scopoletin moieties of the MIP layer. Such interaction was shown to occur between scopoletin as a drug molecule and serum albumins resulting in the formation of scopoletin BSA complexes (Cheng 2012). It is likely that the interaction persists also for polyscopoletin as an inherent property of the polymer film. In the same time the binding of myoglobin

(pI 7.2, MW 16.7 kDa) and Cyt c (pI 10.6, MW 17 kDa) were negligible on the ferritin-imprinted surface. It is interesting to note that the high pI, positively charged Cyt c binds to the negatively charged polymer layer at low ionic strength where electrostatic attraction is effective (data not shown) but the negatively charged ferritin is repulsed by electrostatic forces from the polymer layer in these conditions. However, exactly the opposite occurs at high ionic strength, i.e., Cyt c is no longer bound by electrostatic attraction whilst the elimination of the electrostatic repulsion of ferritin makes the way free for its binding into the MIP cavities.

4. Conclusions

We have shown the feasibility to generate protein-imprinted polymer arrays for protein recognition by microelectrospotting. We confirmed that the polymer spots are compatible with the SPR imaging technique, i.e., the binding properties of the imprinted and non-imprinted polyscopoletin films towards template and interfering proteins could be determined by monitoring the respective interactions simultaneously in real time. Already a rough optimization of ferritin-imprinted MIPs by taking advantage of the multiplexing capabilities of the preparation procedure led to imprinting factor of 13, which is among the highest ever reported for protein MIPs. The ferritin binding was found to be dramatically affected by the ionic strength, which confirms the marked role of electrostatic interactions in protein recognition. The results show that the ionic strength can be used to tune the selectivity of protein MIPs in certain cases and it is a parameter that may worth to consider also during the polymerization. We believe that a more sophisticated microelectrospotting device that is currently under consideration in our labs may lead to high-throughput preparation of protein-imprinted MIPs and their rapid screening. Beside MIP optimization the presented approach may be used to generate MIP arrays as a platform for recognition of various protein panels where the array format might be exploited also as a mean to compensate for contingent cross-reactivities or deficiencies in the selectivity of individual MIPs.

5. Acknowledgement

The financial support of the Lendület program of the Hungarian Academy of Sciences (LP2013-63/2013), and the Hungarian Scientific Fund (K104724) is gratefully acknowledged. F.W.S. gratefully acknowledges the financial support of Deutsche Forschungsgemeinschaft (DFG) within the framework of the German Excellence Initiative (EXC 314), the BMBF in TERA-Sens (93719903) J.W. thanks the German Israeli Foundation for research funding (Grant no. 1074-49.10/2009).

6. References

Bognár, J., Szűcs, J., Dorkó, Z., Horváth, V., Gyurcsányi, R.E., 2013. Nanosphere Lithography as a Versatile Method to Generate Surface-Imprinted Polymer Films for Selective Protein Recognition. Adv. Funct. Mater. 23(37), 4703-4709.

Cai, D., Ren, L., Zhao, H., Xu, C., Zhang, L., Yu, Y., Wang, H., Lan, Y., Roberts, M.F., Chuang, J.H., Naughton, M.J., Ren, Z., Chiles, T.C., 2010. A molecular-imprint nanosensor for ultrasensitive detection of proteins. Nat. Nanotechnol. 5(8), 597-601.

Ceolin, G., Orbán, A., Kocsis, V., Gyurcsányi, R.E., Kézsmárki, I., Horváth, V., 2013. Electrochemical template synthesis of protein-imprinted magnetic polymer microrods. J. Mater. Sci. 48(15), 5209-5218.

Chen, L., Xu, S., Li, J., 2011. Recent advances in molecular imprinting technology: current status, challenges and highlighted applications. Chem. Soc. Rev. 40(5), 2922-2942.

Cheng, Z., 2012. Studies on the interaction between scopoletin and two serum albumins by spectroscopic methods. J. Lumin. 132(10), 2719-2729.

Dechtrirat, D., Gajovic-Eichelmann, N., Bier, F.F., Scheller, F.W., 2014. Hybrid Material for Protein Sensing Based on Electrosynthesized MIP on a Mannose Terminated SelfAssembled Monolayer. Adv. Funct. Mater. 24(15), 2233-2239.

Dechtrirat, D., Jetzschmann, K.J., Stocklein, W.F.M., Scheller, F.W., Gajovic-Eichelmann, N., 2012. Protein Rebinding to a Surface-Confined Imprint. Adv. Funct. Mater. 22(24), 5231-5237.

Dickey, F.H., 1949. The Preparation of Specific Adsorbents. Proc. Natl. Acad. Sci. U.S.A. 35(5), 227-229.

Ge, Y., Turner, A.P.F., 2008. Too large to fit? Recent developments in macromolecular imprinting. Trends Biotechnol. 26(4), 218-224.

Guedon, P., Livache, T., Martin, F., Lesbre, F., Roget, A., Bidan, G., Levy, Y., 2000. Characterization and Optimization of a Real-Time, Parallel, Label-Free, Polypyrrole-Based DNA Sensor by Surface Plasmon Resonance Imaging. Anal. Chem. 72(24), 6003-6009.

Hayden, O., Lieberzeit, P.A., Blaas, D., Dickert, F.L., 2006a. Artificial antibodies for bioanalyte detection-sensing viruses and proteins. Adv. Funct. Mater. 16(10), 1269-1278.

Hayden, O., Mann, K.J., Krassnig, S., Dickert, F.L., 2006b. Biomimetic ABO blood-group typing. Angew. Chem. Int. Edit. 45(16), 2626-2629.

Kempe, M., Glad, M., Mosbach, K., 1995. An approach towards surface imprinting using the enzyme ribonuclease A. Journal of molecular recognition 8(1-2), 35-39.

Lautner, G., Kaev, J., Reut, J., Opik, A., Rappich, J., Syritski, V., Gyurcsányi, R.E., 2011. Selective Artificial Receptors Based on Micropatterned Surface-Imprinted Polymers for Label-Free Detection of Proteins by SPR Imaging. Adv. Funct. Mater. 21(3), 591-597.

Menaker, A., Syritski, V., Reut, J., Opik, A., Horváth, V., Gyurcsányi, R.E., 2009. Electrosynthesized Surface-Imprinted Conducting Polymer Microrods for Selective Protein Recognition. Adv. Mater. 21(22), 2271-2275.

Mercey, E., Grosjean, L., Roget, A., Livache, T., 2007. Surface Plasmon Resonance Imaging on Polypyrrole Protein Chips Microchip-Based Assay Systems. In: Floriano, P.N. (Ed.), pp. 159-175. Humana Press.

Nishino, H., Huang, C.-S., Shea, K.J., 2006. Selective Protein Capture by Epitope Imprinting. Angew. Chem. Int. Edit. 45(15), 2392-2396.

Rachkov, A., Minoura, N., 2000. Recognition of oxytocin and oxytocin-related peptides in aqueous media using a molecularly imprinted polymer synthesized by the epitope approach. J. Chromatogr. A 889(1-2), 111-118.

Saridakis, E., Khurshid, S., Govada, L., Phan, Q., Hawkins, D., Crichlow, G.V., Lolis, E., Reddy, S.M., Chayen, N.E., 2011. Protein crystallization facilitated by molecularly imprinted polymers. Proc. Natl. Acad. Sci. U.S.A. 108(27), 11081-11086.

Schuhmann, W., 1998. Enzyme Biosensors Based on Conducting Polymers. In: Mulchandani, A., Rogers, K. (Eds.), Enzyme and Microbial Biosensors, pp. 143-156. Humana Press.

Shi, H., Tsal, W.B., Garrison, M.D., Ferrari, S., Ratner, B.D., 1999. Template-imprinted nanostructured surfaces for protein recognition. Nature 398(6728), 593-597.

Szeitner, Z., Lautner, G., Nagy, S.K., Gyurcsányi, R.E., Mészáros, T., 2014. A rational approach for generating cardiac troponin I selective Spiegelmers. Chem. Commun. 50(51), 6801-6804.

Villiers, M.-B., Cortès, S., Brakha, C., Marche, P., Roget, A., Livache, T., 2009. Polypyrrole–Peptide Microarray for Biomolecular Interaction Analysis by SPR Imaging Peptide Microarrays. In: Cretich, M., Chiari, M. (Eds.), pp. 317-328. Humana Press.

Vlatakis, G., Andersson, L.I., Muller, R., Mosbach, K., 1993. Drug assay using antibody mimics made by molecular imprinting. Nature 361(6413), 645-647.

Whitcombe, M.J., Chianella, I., Larcombe, L., Piletsky, S.A., Noble, J., Porter, R., Horgan, A., 2011. The rational development of molecularly imprinted polymer-based sensors for protein detection. Chem. Soc. Rev. 40(3), 1547-1571.

Wulff, G., Liu, J., 2012. Design of Biomimetic Catalysts by Molecular Imprinting in Synthetic Polymers: The Role of Transition State Stabilization. Acc. Chem. Res. 45(2), 239-247.

Yildirim, E., Turan, E., Caykara, T., 2012. Construction of myoglobin imprinted polymer films by grafting from silicon surface. J. Mater. Chem. 22(2), 636-642.

Yu, J.C.C., Lai, E.P.C., 2005. Interaction of ochratoxin A with molecularly imprinted polypyrrole film on surface plasmon resonance sensor. React. Funct. Polym. 63(3), 171-176.

Zheng, C., Zhang, X.-L., Liu, W., Liu, B., Yang, H.-H., Lin, Z.-A., Chen, G.-N., 2013. A Selective Artificial Enzyme Inhibitor Based on Nanoparticle-Enzyme Interactions and Molecular Imprinting. Adv. Mater. 25(41), 5922-5927.

Highlights

- First report on using microelectrospotting for electrosynthesis of MIP microarrays
- Ultrathin MIP spots on gold chips allow online SPR imaging of template interactions
- SPR imaging could be used for high throughput readout of MIP arrays
- An imprinting factor of 13 was obtained for optimized ferritin-imprinted MIPs
- The target protein removal and rebinding could be visualized by AFM